

**SYNTHESIS, CHARACTERIZATION, *IN SILICO*  
AND *IN VITRO* EVALUATIONS OF  
BENZIMIDAZOLIUM DERIVED *N*-  
HETEROCYCLIC CARBENES AND THEIR  
SILVER (I)-NHC COMPLEXES**

**NOR FARAH HANI BINTI MD ZIN**

**UNIVERSITI SAINS MALAYSIA**

**2023**

**SYNTHESIS, CHARACTERIZATION, *IN SILICO*  
AND *IN VITRO* EVALUATIONS OF  
BENZIMIDAZOLIUM DERIVED *N*-  
HETEROCYCLIC CARBENES AND THEIR  
SILVER (I)-NHC COMPLEXES**

by

**NOR FARAH HANI BINTI MD ZIN**

**Thesis submitted in fulfilment of the requirements  
for the degree  
Master of Science**

**September 2023**

## ACKNOWLEDGEMENT

First of all, I would like to express my gratitude to Allah S. W. T. for giving me an opportunity and endless strength to complete my research work in fulfilment of the requirements of a MSc degree.

I want to express my gratitude and sincere appreciations to all my family members, especially my beloved mother, Saadiah Mahyuddin for her constant prayers and endless love since the first day I was born. Nothing can be compared to her love and care.

I would like to give my deepest appreciation to my supervisor, Dr. Yam Wan Sinn for her support and advice during this project. I really appreciate her continuous encouragement and guidance during the entire period of my research that had ensured the smooth running of my research. My sincere thanks also goes to my co-supervisor, Assoc. Prof. Dr. Choong Yew Siew, for providing me with the knowledge in molecular modelling and inspiration.

I wish to thank the Malaysian Ministry of Education for providing me with a financial support under the FRGS research grant (FRGS/1/2019/STG01/USM/02/4); the Dean of the School of Chemical Sciences for providing a good research environment and the necessary research facilities; IPS for providing advice and assistance in postgraduate studies-related issues and technical staff of the School of Chemical Science for their help. My gratitude also goes to Khor Boon Keat of the School of Pharmaceutical Sciences for conducting the cytotoxicity assays.

I am so grateful to a bunch of supportive friends, especially Norma, Najah, Umai, Anati, Nabilah and Hawa for their unconditioned support and love. I knew I could always depend and count on you through thick and thin.

## TABLE OF CONTENTS

<b>ACKNOWLEDGEMENT</b> .....	<b>ii</b>
<b>TABLE OF CONTENTS</b> .....	<b>iii</b>
<b>LIST OF TABLES</b> .....	<b>vi</b>
<b>LIST OF FIGURES</b> .....	<b>vii</b>
<b>LIST OF SCHEMES</b> .....	<b>x</b>
<b>LIST OF SYMBOLS AND UNITS</b> .....	<b>xi</b>
<b>LIST OF ABBREVIATIONS</b> .....	<b>xiii</b>
<b>LIST OF APPENDICES</b> .....	<b>xvii</b>
<b>ABSTRAK</b> .....	<b>xxi</b>
<b>ABSTRACT</b> .....	<b>xxiii</b>
<b>CHAPTER 1 INTRODUCTION</b> .....	<b>1</b>
1.1 Background of study .....	1
1.2 Problem statement .....	6
1.3 Research objectives .....	7
<b>CHAPTER 2 LITERATURE REVIEW</b> .....	<b>8</b>
2.1 Introduction to carbenes .....	8
2.2 N-heterocyclic carbenes (NHCs) .....	10
2.3 Synthesis of azolium salts: the NHC precursors .....	13
2.3.1 Condensation-reduction route .....	13
2.3.2 Nucleophilic substitution at the azole heterocycles .....	14
2.4 Benzimidazoles as NHC precursors .....	15
2.5 Metal-NHC complexes .....	17
2.6 Preparations of metal-NHC complexes .....	17
2.6.1 <i>In situ</i> deprotonation of azolium salts .....	17

2.6.2	Reaction of free carbenes with metal precursors .....	20
2.6.3	Transmetalation or carbene transfer .....	20
2.7	Silver(I) NHC complexes.....	21
2.7.1	Antimicrobial activities of Ag(I)-NHC complexes.....	22
2.7.2	Anticancer activities of Ag(I)-NHC complexes .....	24
2.8	Mechanism of action of Ag(I)-NHC complexes .....	26
2.8.1	Caspase-dependent apoptotic pathway.....	27
2.8.2	Caspase-independent apoptotic pathway .....	28
2.8.3	DNA pathway .....	28
2.9	Possible/ promising protein targets .....	30
2.9.1	Selenoenzyme thioredoxin reductase (TrxR).....	30
2.9.2	Gold(I)- and Ag(I)-NHC complexes as TrxR inhibitors .....	31
2.10	Molecular modelling .....	34
2.10.1	Molecular docking.....	34
	2.10.1(a) Search algorithms .....	35
	2.10.1(b) Scoring functions .....	35
	<b>CHAPTER 3 METHODOLOGY .....</b>	<b>37</b>
3.1	Chemicals and materials.....	37
3.2	Instruments .....	38
3.3	Synthesis.....	39
3.4	Synthesis of <i>N</i> -alkyl- <i>N</i> -methyl/octadecyl benzimidazolium bromides .....	40
3.4.1	Synthesis of <i>N</i> -alkyl- <i>N</i> '-methyl benzimidazolium bromides, <b>1-5</b> .....	40
3.4.2	Synthesis of <i>N</i> -alkyl- <i>N</i> '-octadecyl benzimidazolium bromides, <b>6-13</b> .....	42
3.5	Synthesis of <i>N</i> -alkyl- <i>N</i> '-methyl/octadecyl-benzimidazol-2-ylidene silver(I) hexafluorophosphate .....	46

3.5.1	Synthesis of <i>N</i> -alkyl- <i>N</i> '-methyl benzimidazol-2-ylidene silver(I) hexafluorophosphates, <b>14-18</b> .....	47
3.5.2	Synthesis of <i>N</i> -alkyl- <i>N</i> '-octadecyl benzimidazol-2-ylidene silver(I) hexafluorophosphates, <b>19-25</b> .....	50
3.6	Density Functional Theory (DFT).....	53
3.7	Cell lines and culture conditions .....	54
3.8	Molecular docking .....	55
3.8.1	Protein target and ligands preparation.....	55
3.8.2	Docking and scoring protocol .....	55
<b>CHAPTER 4 RESULTS AND DISCUSSION .....</b>		<b>57</b>
4.1	Synthesis.....	57
4.2	Spectral analysis .....	57
4.2.1	Fourier-transform infrared spectroscopy analysis .....	57
4.2.2	<sup>1</sup> H- and <sup>13</sup> C- NMR spectroscopy analysis .....	60
4.3	Cytotoxicity studies.....	76
4.4	Theoretical geometries and binding enthalpies of complex <b>16</b> .....	81
4.5	Binding affinities and molecular interaction of ligand 1-3 and TrxR.....	85
<b>CHAPTER 5 CONCLUSION AND FUTURE RECOMMENDATIONS .....</b>		<b>90</b>
5.1	Conclusion.....	90
5.2	Recommendations for future research.....	92
<b>REFERENCES.....</b>		<b>93</b>
<b>APPENDICES</b>		
<b>LIST OF PUBLICATIONS</b>		

## LIST OF TABLES

	<b>Page</b>
Table 4.1	<sup>1</sup> H- <sup>1</sup> H correlations as inferred from 2D COSY NMR spectral analysis for compound <b>3</b> . .....61
Table 4.2	<sup>1</sup> H- <sup>13</sup> C correlations as inferred from 2D HSQC and HMBC spectral analysis for compound <b>3</b> . .....67
Table 4.3	<sup>1</sup> H- <sup>1</sup> H correlations as inferred from 2D COSY NMR spectral analysis for compound <b>16</b> . .....69
Table 4.4	<sup>1</sup> H- <sup>13</sup> C correlations as inferred from 2D HSQC and HMBC spectral analysis for compound <b>16</b> . .....75
Table 4.5	The half maximal inhibitory concentrations (IC <sub>50</sub> ) and selectivity indices of the ligands, <b>1-13</b> and their silver(I)-NHC complexes, <b>14-25</b> on HeLa and Hs-27 cells at 24 h as determined using the MTT assay. Etoposide was used as the control drug.....76
Table 4.6	Binding energies, inhibition constants and interactions of <b>1-13</b> and TrxR1.. .....85

## LIST OF FIGURES

	<b>Page</b>
Figure 1.1	The three benzimidazole derived anticancer drugs, binimetinib, bendamustine and galeterone (Purushottamachar <i>et al.</i> , 2019). ..... 3
Figure 1.2	Bioactive <i>N</i> -Allyl- <i>N'</i> -substituted benzimidazolium chlorides (Cevik <i>et al.</i> , 2020). ..... 4
Figure 2.1	A general structure of a carbene. .... 8
Figure 2.2	Electron spin in (a) a singlet carbene, and (b) a triplet carbene ..... 9
Figure 2.3	Carbene to metal bonding in (a) Fisher carbenes (Fischer and Maasböl, 1964) (b) Schrock carbenes (Schrock, 1974). ..... 10
Figure 2.4	Stabilisation of NHCS via resonance and negative inductive effects (Bourissou <i>et al.</i> , 2000; Boehme & Frenking <i>et al.</i> , 1996). ..... 12
Figure 2.5	Benzimidazole tautomers..... 16
Figure 2.6	Benzimidazole derivatives with different N-substituents (Min <i>et al.</i> , 2019). ..... 16
Figure 2.7	Silver sulfadiazine, a topical antibiotic..... 22
Figure 2.8	Bioactive benzimidazolium derived silver(I)-NHC complexes, <b>9a-9c</b> (Kaloğlu, <i>et al.</i> , 2016)..... 24
Figure 2.9	Imidazolium derived silver(I)-NHC complexes with anticancer properties (Youngs <i>et al.</i> , 2005)..... 24
Figure 2.10	1-Allyl benzimidazolium silver(I)-NHC complexes, <b>13a-13d</b> (Sahin <i>et al.</i> , 2019)..... 25
Figure 2.11	Morphine-linked benzimidazolium derived silver(I)-NHC complexes, <b>14a-14c</b> which induced apoptosis via a caspase-dependent pathway (Kutlu <i>et al.</i> , 2021)..... 27



Figure 2.12	Figure 2.12: Ag(I)-NHC complexes, <b>15a-15c</b> induced caspase-independent apoptosis (Eloy et al., 2012).....	28
Figure 2.13	Imidazolium metal-NHC complexes with different binding modes, <b>16a-16b</b> (Guarra et al., 2021)..	29
Figure 2.14	The 3D representation of a human homodimeric TrxR enzyme, hTrxR1 (Protein Data Bank entry: 2J3N).....	30
Figure 2.15	Mono and bis Au(II)-NHC complexes as TrxR inhibitors (Rubbiani et al., 2011)....	32
Figure 2.16	Halogenated and non- halogenated gold(I)-NHC complexes, <b>18a-18h</b> (Schmidt <i>et al.</i> , 2017).....	33
Figure 2.17	TrxR inhibitors derived from gold(I) and silver(I)-NHC complexes (Citta <i>et al.</i> , 2013).....	34
Figure 4.1	Spectra of ligand <b>3</b> (top) and its corresponding silver(I)-NHC complex <b>16</b> (bottom).....	59
Figure 4.2	<sup>1</sup> H NMR spectrum of compound <b>3</b> (in DMSO).....	61
Figure 4.3	<sup>1</sup> H- <sup>1</sup> H COSY spectrum of <b>3</b> .....	62
Figure 4.4	<sup>13</sup> C NMR spectrum of compound <b>3</b> (in DMSO).....	64
Figure 4.5	<sup>1</sup> H- <sup>13</sup> C HSQC spectrum of <b>3</b> .....	65
Figure 4.6	<sup>1</sup> H- <sup>13</sup> C HMBC spectrum of <b>3</b> .....	66
Figure 4.7	Expanded <sup>1</sup> H- <sup>13</sup> C HMBC spectrum of <b>3</b> (7.80-8.50 ppm; 130.0-134.0 ppm).....	67
Figure 4.8	<sup>1</sup> H NMR spectrum of compound <b>16</b> (in CDCl <sub>3</sub> ).....	69
Figure 4.9	<sup>1</sup> H- <sup>1</sup> H COSY spectrum of <b>16</b> .....	70
Figure 4.10	<sup>13</sup> C NMR spectrum of compound <b>16</b> (in CDCl <sub>3</sub> ).....	72
Figure 4.11	<sup>1</sup> H- <sup>13</sup> C HSQC spectrum of <b>16</b> .....	73
Figure 4.12	<sup>1</sup> H- <sup>13</sup> C HMBC spectrum of <b>16</b> .....	74

Figure 4.13	Geometries of lowest energy [Ag(NHC) <sub>2</sub> ] <sup>+</sup> complexes of (a) <b>16A</b> and dissociation complex of (b) <b>16B</b> optimized at M06 level of theory. Non-covalent interactions evaluated at a density cut off of 0.05 au are shown as green surfaces..... 77
Figure 4.14	The overall binding enthalpies ΔH° <sub>298</sub> of 16A (black fonts) are dissected into two major components, namely Ag...C bond strength (blue fonts) and NC-I of side chains (red fonts)..... 78
Figure 4.15	The cytotoxicity of ligands <b>1-5</b> against HeLa and Hs27 cells. The compounds showed dose-dependent manner in reduction of cell viability..... 81
Figure 4.16	The cytotoxicity of ligands <b>6-11</b> against HeLa and Hs27 cells. The compounds showed dose-dependent manner in reduction of cell viability..... 81
Figure 4.17	The cytotoxicity of silver(I)-NHC complexes, <b>14-18</b> against HeLa and Hs27 cells. The compounds showed dose-dependent manner in reduction of cell viability..... 82
Figure 4.18	The cytotoxicity of silver(I)-NHC complexes, <b>19-24</b> against HeLa and Hs27 cells. The compounds showed dose-dependent manner in reduction of cell viability..... 84
Figure 4.19	The best predicted binding poses of (top) etoposide and (bottom) ligand <b>1</b> in the binding site of TrxR-1..... 88

## LIST OF SCHEMES

	<b>Page</b>
Scheme 2.1	Formation of a dimeric NHC, entatramine, <b>2</b> from N, N'-disubstituted imidazolidine, <b>1</b> (Wanzlik <i>et al.</i> , 1960)..... 11
Scheme 2.2	The first isolable free NHC (Arduengo <i>et al.</i> , 1991)..... 12
Scheme 2.3	Symmetric synthesis of imidazolium salts (Bohm <i>et al.</i> , 2000). ..... 13
Scheme 2.4	Asymmetric synthesis of imidazolium salts (Gridney & Mihaltaseva, 2000).. ..... 14
Scheme 2.5	Synthesis of symmetrical or asymmetrical benzimidazolium salts (Starikova <i>et al.</i> , 2003). ..... 15
Scheme 2.6	Synthesis of the first NHC-transition metal complexes by (a) Wanzilk and (b) Öfele. .... 18
Scheme 2.7	In situ deprotonation of azolium salts by Ag <sub>2</sub> O to form silver(I)-NHC complexes (Wang & Lin, 1998)..... 19
Scheme 2.8	Synthesis of bis silver(I)-NHC complexes using a basic phase transfer catalyst (Tulloch <i>et al.</i> , 1968)..... 19
Scheme 2.9	Synthesis of the first silver(I)-NHC complex from 1,3-dimesitylimidazol-2-ylidene and silver(I)triflate (Arduengo, 1993). ..... 20
Scheme 2.10	Transmetalation reaction from a W(0)-NHC complex to Au(I)-NHC complex (Ku <i>et al.</i> , 1999)..... 21
Scheme 2.11	Synthesis of <b>7a-b</b> and <b>8a-b</b> from 2,6-bis(imidazolomethyl)pyridine (Youngs, <i>et al.</i> , 2004)..... 23
Scheme 2.12	Synthesis of <i>N,N'</i> -dialkylatedbenzimidazole-based NHC ligands, <b>11a-11h</b> and their silver (I)-complexes, <b>12a-12h</b> (Fatima <i>et al.</i> , 2017)..... 25
Scheme 3.1	Synthesis of benzimidazolium salts, <b>1-13</b> and silver(I)-NHC complexes, <b>14-25</b> ..... 39

## LIST OF SYMBOLS AND UNITS

Å	Angstrom
g	Gram
g/mol	Gram per mole
Hz	Hertz
h	Hour
Kcal	Kilocalorie
m/z	Mass-to-charge ratio
MHz	Megahertz
µg	Microgram
µL	Microlitre
µM	Micromolar
µm	Micrometre
mg	Milligram
mL	Millilitre
mol	Mole
mmol	Millimole
min	Minute
Nm	Nanometre
%	Percentage
cm <sup>-1</sup>	Per centimetre
°C	Degree Celsius
δ	Chemical shift
σ	Sigma

ppm	Parts per million
<i>J</i>	Coupling constant
v/v	Volume/volume ratio
w/w	Weight/weight ratio
$\nu$	Wavenumber
V	Volt
%	Percentage
$\pi$	Pi

## LIST OF ABBREVIATIONS

Ag <sup>+</sup>	Silver ions
AgOAc	Silver acetate
Ag <sub>2</sub> O <sub>3</sub>	Silver carbonate
Ag <sub>2</sub> O	Silver(I) oxide
Ag(I)-NHC	Silver(I)- <i>N</i> -heterocyclic carbene complexes
AgBr	Silver bromide
Ar	Aromatic
Au(I)	Gold(I)
Au(I)-NHC	Gold(I)- <i>N</i> -heterocyclic carbene complexes
AIF	Apoptosis-inducing factor
Anal.	Analysis
AR	Analytical reagent
BCNU	Carmustine
BSA	Serum albumin protein
C	Aliphatic chain length
<sup>13</sup> C-NMR	Carbon-13 nuclear magnetic resonance
Cald.	Calculated
CAgF <sub>3</sub> O <sub>3</sub> S	Silver(I) triflate
CADD	Computer-aided drug design
CAPAN-1	Adenocarcinoma cell lines
CHN	Carbon nitrogen hydrogen
Cu(I)-NHC	Copper(I)- <i>N</i> -heterocyclic carbene
d	Doublet
1D	One-dimesional

2D	Two-dimensional
DEPT	Distortionless enhancement by polarization transfer
DFT	Density functional theory
DMSO	Dimethyl sulfoxide
DMEM	Dulbecco's Modified Eagles's Medium
DNA	Deoxyribonucleic acid
EC <sub>50</sub>	Half minimal effective concentration
<i>E. coli</i>	<i>Eschericia coli</i>
FAD	Flavin adenin
FBS	Fetal bovine serum
FDA	Food and Drug Administration
FTIR	Fourier-transform infrared
GA	Genetic algorithm
GLOBOCAN	Global Cancer Observatory
<sup>1</sup> H-NMR	Hydrogen-1 nuclear magnetic resonance
H	Hydrogen
HCT-116	Colon cancer cell lines
HeLa	Cervical cancer cell lines
Hs27	Human skin fibroblast cell lines
HgOAc	Mercury(II) acetate
Hg(II)-NHC	Mercury(II)- <i>N</i> -heterocyclic carbene
IC <sub>50</sub>	Half maximal inhibitory concentration
IUPAC	International Union of Pure and Applied Chemistry
<i>K<sub>i</sub></i>	Inhibition constant
KH	Potassium hydride

KOH	Potassium hydroxide
KotBu	Potassium tert-butoxide
Kda	Kilodalton
KPF <sub>6</sub>	Potassium Hexafluorophosphate
LBDD	Ligand-based drug design
LGA	Lamarckian genetic algorithm
m	Multiplets
metal-NHC	Metal- <i>N</i> -heterocyclic carbene
MB-231	Breast cancer cell lines
MB-157	Breast cancer cell lines
MDA-MB-231	Breast cancer cell lines
MDA-MB-436	Breast cancer cell lines
MCF-7	Breast cancer cell lines
MIC	Minimum inhibitory concentration
MD	Molecular docking
MEOH	Methanol
MeCN	Acetonitrile
MTT	3-(4,5-Dimethylthiazol-2-yl)-2,5-diphenyltetrazolium
N	Nitrogen
NADPH	Nicotinamide adenine dinucleotide phosphate hydrogen
NaH	Sodium hydride
NCI	Non-covalent interaction
NHC	<i>N</i> -heterocyclic carbene
NMR	Nuclear magnetic resonance
OVCAR-3	Ovarian cancer-3
PARP-1	Poly(ADP-ribose) polymerase-1



Pd-NHC	Palladium- <i>N</i> -Heterocyclic carbene
PDB	Protein data bank
PCM	Polarisable continuum model
PES	Potential energy surfaces
<i>P. aeruginosa</i>	<i>Pseudomonas aeruginosa</i>
quint	Quintet
RCSB	Research Collaboratory for Bioinformatics
s	Singlet
SBDD	Structure-based drug design
SDD	Stuttgart-Dresden
t	Triplet
THF	Tetrahydrofuran
TLC	Thin layer chromatography
TrxR	Thioredoxin reductase
TrxR-1	Cytosolic thioredoxin reductase
TrxR-2	Mitochondrial thioredoxin reductase
UV	Ultraviolet
VMD	Visual molecular dynamic
W(0)-NHC	Tungsten(0)- <i>N</i> -Heterocyclic carbene
ZPVE	Zero-point vibration energies

## LIST OF APPENDICES

Appendix 1	FT-IR spectrum of compound <b>1</b>
Appendix 2	FT-IR spectrum of compound <b>2</b>
Appendix 3	FT-IR spectrum of compound <b>3</b>
Appendix 4	FT-IR spectrum of compound <b>4</b>
Appendix 5	FT-IR spectrum of compound <b>5</b>
Appendix 6	FT-IR spectrum of compound <b>6</b>
Appendix 7	FT-IR spectrum of compound <b>7</b>
Appendix 8	FT-IR spectrum of compound <b>8</b>
Appendix 9	FT-IR spectrum of compound <b>9</b>
Appendix 10	FT-IR spectrum of compound <b>10</b>
Appendix 11	FT-IR spectrum of compound <b>11</b>
Appendix 12	FT-IR spectrum of compound <b>12</b>
Appendix 13	FT-IR spectrum of compound <b>13</b>
Appendix 14	FT-IR spectrum of compound <b>14</b>
Appendix 15	FT-IR spectrum of compound <b>15</b>
Appendix 16	FT-IR spectrum of compound <b>16</b>
Appendix 17	FT-IR spectrum of compound <b>17</b>
Appendix 18	FT-IR spectrum of compound <b>18</b>
Appendix 19	FT-IR spectrum of compound <b>19</b>
Appendix 20	FT-IR spectrum of compound <b>20</b>
Appendix 21	FT-IR spectrum of compound <b>21</b>
Appendix 22	FT-IR spectrum of compound <b>22</b>
Appendix 23	FT-IR spectrum of compound <b>23</b>
Appendix 24	FT-IR spectrum of compound <b>24</b>

Appendix 25	FT-IR spectrum of compound <b>25</b>
Appendix 26	$^1\text{H}$ NMR spectrum of compound <b>1</b> (in DMSO- $d_6$ )
Appendix 27	$^{13}\text{C}$ NMR spectrum of compound <b>1</b> (in DMSO- $d_6$ )
Appendix 28	$^1\text{H}$ NMR spectrum of compound <b>2</b> (in DMSO- $d_6$ )
Appendix 29	$^{13}\text{C}$ NMR spectrum of compound <b>2</b> (in DMSO- $d_6$ )
Appendix 30	$^1\text{H}$ NMR spectrum of compound <b>3</b> (in DMSO- $d_6$ )
Appendix 31	$^{13}\text{C}$ NMR spectrum of compound <b>3</b> (in DMSO- $d_6$ )
Appendix 32	$^1\text{H}$ NMR spectrum of compound <b>4</b> (in DMSO- $d_6$ )
Appendix 33	$^{13}\text{C}$ NMR spectrum of compound <b>4</b> (in DMSO- $d_6$ )
Appendix 34	$^1\text{H}$ NMR spectrum of compound <b>5</b> (in DMSO- $d_6$ )
Appendix 35	$^{13}\text{C}$ NMR spectrum of compound <b>5</b> (in DMSO- $d_6$ )
Appendix 36	$^1\text{H}$ NMR spectrum of compound <b>6</b> (in $\text{CD}_3\text{OD}$ )
Appendix 37	$^{13}\text{C}$ NMR spectrum of compound <b>6</b> (in $\text{CD}_3\text{OD}$ )
Appendix 38	$^1\text{H}$ NMR spectrum of compound <b>7</b> (in $\text{CD}_3\text{OD}$ )
Appendix 39	$^{13}\text{C}$ NMR spectrum of compound <b>7</b> (in $\text{CD}_3\text{OD}$ ).
Appendix 40	$^1\text{H}$ NMR spectrum of compound <b>8</b> (in $\text{CD}_3\text{OD}$ )
Appendix 41	$^{13}\text{C}$ NMR spectrum of compound <b>8</b> (in $\text{CD}_3\text{OD}$ )
Appendix 42	$^1\text{H}$ NMR spectrum of compound <b>9</b> (in $\text{CDCl}_3$ )
Appendix 43	$^{13}\text{C}$ NMR spectrum of compound <b>9</b> (in $\text{CDCl}_3$ )
Appendix 44	$^1\text{H}$ NMR spectrum of compound <b>10</b> (in $\text{CDCl}_3$ )
Appendix 45	$^{13}\text{C}$ NMR spectrum of compound <b>10</b> (in $\text{CDCl}_3$ )
Appendix 46	$^1\text{H}$ NMR spectrum of compound <b>11</b> (in $\text{CDCl}_3$ )
Appendix 47	$^{13}\text{C}$ NMR spectrum of compound <b>11</b> (in $\text{CDCl}_3$ )
Appendix 48	$^1\text{H}$ NMR spectrum of compound <b>12</b> (in $\text{CDCl}_3$ )
Appendix 49	$^{13}\text{C}$ NMR spectrum of compound <b>12</b> (in $\text{CDCl}_3$ )
Appendix 50	$^1\text{H}$ NMR spectrum of compound <b>13</b> (in $\text{CDCl}_3$ )

Appendix 51	$^{13}\text{C}$ NMR spectrum of compound <b>13</b> (in $\text{CDCl}_3$ )
Appendix 52	$^1\text{H}$ NMR spectrum of compound <b>14</b> (in $\text{CDCl}_3$ )
Appendix 53	$^{13}\text{C}$ NMR spectrum of compound <b>14</b> (in $\text{CDCl}_3$ )
Appendix 54	$^1\text{H}$ NMR spectrum of compound <b>15</b> (in $\text{CDCl}_3$ )
Appendix 55	$^{13}\text{C}$ NMR spectrum of compound <b>15</b> (in $\text{CDCl}_3$ )
Appendix 56	$^1\text{H}$ NMR spectrum of compound <b>16</b> (in $\text{CDCl}_3$ )
Appendix 57	$^{13}\text{C}$ NMR spectrum of compound <b>16</b> (in $\text{CDCl}_3$ )
Appendix 58	$^1\text{H}$ NMR spectrum of compound <b>17</b> (in $\text{CDCl}_3$ )
Appendix 59	$^{13}\text{C}$ NMR spectrum of compound <b>17</b> (in $\text{CDCl}_3$ )
Appendix 60	$^1\text{H}$ NMR spectrum of compound <b>18</b> (in $\text{CDCl}_3$ )
Appendix 61	$^{13}\text{C}$ NMR spectrum of compound <b>18</b> (in $\text{CDCl}_3$ )
Appendix 62	$^1\text{H}$ NMR spectrum of compound <b>19</b> (in $\text{CD}_3\text{OD}$ )
Appendix 63	$^{13}\text{C}$ NMR spectrum of compound <b>19</b> (in $\text{CD}_3\text{OD}$ )
Appendix 64	$^1\text{H}$ NMR spectrum of compound <b>20</b> (in $\text{CD}_3\text{OD}$ )
Appendix 65	$^{13}\text{C}$ NMR spectrum of compound <b>20</b> (in $\text{CD}_3\text{OD}$ )
Appendix 66	$^1\text{H}$ NMR spectrum of compound <b>21</b> (in $\text{CD}_3\text{OD}$ )
Appendix 67	$^{13}\text{C}$ NMR spectrum of compound <b>21</b> (in $\text{CDCl}_3$ )
Appendix 68	$^1\text{H}$ NMR spectrum of compound <b>22</b> (in $\text{CDCl}_3$ )
Appendix 69	$^{13}\text{C}$ NMR spectrum of compound <b>22</b> (in $\text{CDCl}_3$ )
Appendix 70	$^1\text{H}$ NMR spectrum of compound <b>23</b> (in $\text{CDCl}_3$ )
Appendix 71	$^{13}\text{C}$ NMR spectrum of compound <b>23</b> (in $\text{CDCl}_3$ )
Appendix 62	$^1\text{H}$ NMR spectrum of compound <b>24</b> (in $\text{CDCl}_3$ )
Appendix 73	$^{13}\text{C}$ NMR spectrum of compound <b>24</b> (in $\text{CDCl}_3$ )
Appendix 74	$^1\text{H}$ NMR spectrum of compound <b>25</b> (in $\text{CDCl}_3$ )
Appendix 75	$^{13}\text{C}$ NMR spectrum of compound <b>25</b> (in $\text{CDCl}_3$ )
Appendix 76	$^{13}\text{C}$ -DEPT45 NMR spectrum of compound <b>3</b> (in $\text{DMSO-d}_6$ )

- Appendix 77  $^{13}\text{C}$ -DEPT90 NMR spectrum of compound **3** (in DMSO- $d_6$ )
- Appendix 78  $^{13}\text{C}$ -DEPT135 NMR spectrum of compound **3** (in DMSO- $d_6$ )
- Appendix 79  $^{13}\text{C}$ -DEPT45 NMR spectrum of compound **16** (in  $\text{CDCl}_3$ )
- Appendix 80  $^{13}\text{C}$ -DEPT90 NMR spectrum of compound **16** (in  $\text{CDCl}_3$ )
- Appendix 81  $^{13}\text{C}$ -DEPT135 NMR spectrum of compound **25** (in  $\text{CDCl}_3$ )

**SINTESIS, PENCIRIAN, PENILAIAN *IN SILICO* DAN *IN VITRO* N-  
HETEROSIKLIK KARBENA BERASASKAN BENZIMIDAZOLIUM DAN  
KOMPLEKS ARGENTUM (I)-NHC**

**ABSTRAK**

Dalam kajian ini, dua siri ligan *N*-heterosiklik karbena (NHC) berasaskan benzimidazolium dan kompleks Ag(I)-NHC telah disintesis dan dicirikan dengan spektroskopi Fourier-transform inframerah (FT-IR), spektroskopi Fourier-transform nuklear magnetik resonan (FT-NMR), dan analisis unsur CHN. Ligan, **1-13** telah disintesis melalui tindak balas pengalkian antara 1-metil/oktadesilbenzimidazolium dengan benzil bromida (C = 4-18, dalam pariti genap). Ligan tersebut ditindakbalas dengan argentum oksida (Ag<sub>2</sub>O) melalui deprotonasi *in situ*, diikuti dengan tindak balas metatesis dengan kalium heksafluorofosfat (KPF<sub>6</sub>) untuk menghasilkan kompleks Ag(I)-NHC, **14-25**. Tenaga bebas pengikatan ( $\Delta G$ ), pemalar perencatan ( $K_i$ ) dan interaksi ligan **1-13** dengan enzim seleno thioeredoksin reduktase (TrxR) telah dikaji oleh dok molekul. Sitotoksisiti *in vitro* semua sebatian, **1-25** terhadap sel kanser serviks (HeLa) dan sel kanser fibroblast manusia (Hs27) telah dikaji menggunakan ujian MTT. Panjang rantai alkil pada atom nitrogen dalam bahagian benzimidazolium dan kehadiran ion Ag<sup>+</sup>, mempengaruhi sitotoksisiti sebatian ini. Sitotoksisiti sebatian ini meningkat dengan peningkatan panjang rantai alkil. Bagi ligan, homolog rantai panjang, **9-11** (C10-C14) adalah lebih sitotoksik (IC<sub>50</sub> = 1.35-12.68 $\mu$ M) dan selektif terhadap sel HeLa berbanding dengan analog rantai pendek, **1-4** (IC<sub>50</sub> = 3.53-35 $\mu$ M). Kehadiran ion Ag<sup>+</sup> telah meningkatkan sitotoksisiti kompleks rantai pendek, **14-18** dengan ketara, tetapi pada tahap yang lebih rendah dalam analog rantai panjang, **19-**

**21**, namun kesan ini hilang dalam kompleks **22-25**. Sitotoksiti ligan, **1-11** dan kompleks, **14-24** terhadap sel HeLa ( $IC_{50} = 1.18-2.79 \mu M$ ) adalah lebih tinggi berbanding dengan sitotoksiti etoposide ( $IC_{50} = 25.67 \mu M$ ). Pengiraan teori fungsi ketumpatan mendedahkan bahawa geometri kompleks **16** yang paling stabil ialah geometri hampir linear dengan sudut C–Ag–C kira-kira  $171^{\circ}$ - $173^{\circ}$ . Pusat Ag adalah terikat kepada dua atom karbena daripada dua ligan NHC. Interaksi bukan kovalen antara rantai alkil yang panjang membentuk kira-kira satu pertiga daripada jumlah tenaga pengikatan. Tetapi, keputusan dok molekul dan kesan sitotoksik tidak berhubungkait dengan baiknya. Ligan rantai panjang, **6-12** yang mempunyai nilai pemalar perencatan yang jauh lebih besar ( $K_i = 20.31-38.99 \text{ nM}$ ) adalah banyak kali lebih sitotoksik berbanding dengan analog rantai pendek yang sepadan, **1-5** ( $K_i = 6.49-15.32 \text{ nM}$ ). Ini menunjukkan bahawa walaupun dok molekul ialah suatu kaedah *in silico* yang digunakan untuk mengkaji interaksi ligan-protein, ia tidak memberikan ramalan tenaga atau geometrik yang dapat memberikan anggaran termodinamik dan kinetik yang lebih tepat tentang pencaman dan pengikatan sasaran dadah.

**SYNTHESIS, CHARACTERIZATION, *IN SILICO* AND *IN VITRO***  
**EVALUATIONS OF BENZIMIDAZOLIUM DERIVED *N*-HETEROCYCLIC**  
**CARBENES AND THEIR SILVER (I)-NHC COMPLEXES**

**ABSTRACT**

Two new series of asymmetrical benzimidazolium-based *N*-heterocyclic carbene (NHC) ligands and their Ag(I)-NHC complexes were synthesised and characterised using Fourier-transform infrared (FTIR) and Fourier-transform nuclear magnetic resonance (FT-NMR) spectroscopies and CHN elemental analysis. The ligands, **1-13** were synthesized *via* alkylation of 1-methyl/octadecylbenzimidazole with alkyl bromides (C = 4-18 in even parity), These ligands were reacted with silver oxide (Ag<sub>2</sub>O) *via in situ* deprotonation reaction, followed by metathesis reaction with potassium hexafluorophosphate (KPF<sub>6</sub>) to yield Ag(I)-NHC complexes, **14-25**. The binding free energies ( $\Delta G$ ), inhibition constants ( $K_i$ ) and the interactions of ligands **1-13** and selenoenzyme thioredoxin reductase (TrxR) were predicted using molecular docking. The *in vitro* cytotoxicity of all compounds, **1-25** against human cervical cancer cells (HeLa) and human skin fibroblasts (Hs27) were evaluated using the MTT assay. The length of alkyl chains on nitrogen atoms in the benzimidazolium moiety, as well as the presence of Ag<sup>+</sup> ions, influenced the cytotoxicity of these compounds. Cytotoxicity of these compounds increased with increasing alkyl chain length. For ligands, the long-chain homologues, **9-11** (C10-C14) were more potent (IC<sub>50</sub> = 1.35-12.68  $\mu$ M) and selective than the short-chain analogues, **1-4** (IC<sub>50</sub> = 3.53-35  $\mu$ M) against HeLa cells. The presence of Ag<sup>+</sup> ions significantly enhanced the cytotoxicity of the short-chain complexes, **14-18** but to a lesser extent in the long-chain analogues,



**19-21**, but this effect was lost in complexes **22-25**. Cytotoxicity of the ligands, **1-11** and complexes, **14-24** against HeLa cells ( $IC_{50} = 1.18-2.79 \mu M$ ) was superior to that of etoposide ( $IC_{50} = 25.67 \mu M$ ). Density functional theory calculations revealed that the most stable geometry of complex **16** has an almost linear geometry with the C–Ag–C angle of about  $171^\circ-173^\circ$ . The Ag centre is bonded to two carbene atoms of the two NHC ligands. The non-covalent interactions between the long alkyl chains made up about one-third of the total binding energy. The molecular docking results, however, did not correlate well with cytotoxic effects. The long-chain ligands, **6-12** with much larger inhibition constants ( $K_i = 20.31 -38.99 \text{ nM}$ ) were many folds more cytotoxic compared to the corresponding short-chain analogues, **1-5** ( $K_i = 6.49-15.32 \text{ nM}$ ). This shows that although molecular docking is a common *in silico* method used to study ligand-protein interaction, it does not give energetic or geometric predictions which are useful in providing a more accurate estimation of the thermodynamics and kinetics associated with drug-target recognition and binding.

## CHAPTER 1

### INTRODUCTION

#### 1.1 Background of study

Cancer refers to a group of disease in a living organism in which the aberrant cells develop uncontrollably and attack other cells in the body. The worldwide rise in cancer rates is very concerning. By 2040, the number of cancer cases in Malaysia is anticipated to increase, from 43,837 to 84,158 cases ("Global Cancer Observatory", 2018). Cancer is a highly complicated and invasive disease characterised by continuous proliferative signalling, infinite replicative potential, and the risk of metastasis (Hanahan & Weinberg Robert, 2011). Among various types of cancer, cervical cancer is the fourth most common cancer in woman globally (Arbyn *et al.*, 2020; Bray *et al.*, 2018) and the second most common and deadly gynaecological cancer in low- and middle-income countries (LMICs) (Kafuruki *et al.*, 2013).

Since Rosenberg and co-workers discovered cisplatin, metallopharmaceuticals have played an important role in cancer chemotherapy (Rosenberg 1967; Johnstone, *et al.*, 2014). Today, a number of platinum complexes, such as oxaliplatin, carboplatin, nedaplatin, and lobaplatin are used in tumour therapy (Hang *et al.*, 2016). However, platinum-based chemotherapeutics could only be used to treat a small percentage of cancers, and patients frequently experience side effects such as vomiting, nausea, decrease in blood cell counts and platelet counts, neurotoxicity, and nephrotoxicity (Liu *et al.*, 2013). Consequently, it is very important for researchers to design and develop efficient and safe anticancer medicines from alternative transition metal complexes with enhanced organic ligands.

Many organometallic chemists find the molecule carbene, which is a divalent carbon species with two unpaired electrons, to be of great interest (Kirmse, 2004). Due to the existence of unpaired electrons, carbenes are very reactive. They are excellent nucleophiles and strong Lewis bases which can bind with metal ions across the periodic table to form highly stable complexes. Hence, carbenes are usually used as intermediates in synthetic chemistry (Liu *et al.*, 2021). Over the last few decades, *N*-heterocyclic carbenes (NHCs) had piqued academic and commercial attention. These cyclic compounds, which contain at least one nitrogen atom bound to a divalent carbon atom inside the heterocycles, are an interesting class of organic ligands which are stable, easy to prepare and isolate. 1,3-di-1-adamantyl-imidazol-2-ylidene was the first stable crystalline NHC isolated by Arduengo and co-workers in 1991. NHCs have high potential to form very stable complexes with transition metals due to  $\pi$ -donation and  $\sigma$ -electronegativity effects, including the steric hindrance (Patil *et al.*, 2011). At low and high oxidation states, NHCs are good  $\sigma$ -donors to transition metals. Many of these ligands are used as precursors in drug development, thus allowing tuning of their physicochemical and biological properties (Gasser *et al.*, 2011).

Benzimidazole is an essential heterocyclic moiety in medicines. The bioactivities of the benzimidazole ring are intrinsically linked to its structural resemblance to some naturally occurring compounds, such as purines. Purines are the building blocks of nucleic acids and can easily interact with biomolecules in the ecosystems (Sharma *et al.*, 2012). To date, many benzimidazole derivatives have been reported to show antiviral (De Clercq & Naesens, 2006), antibacterial (Ozkey *et al.*, 2011), anti-human deficiency virus (HIV) (Dayam *et al.*, 2006), and anti-hepatic (Ishida *et al.*, 2006) activities. In particular, benzimidazole derivatives had significant therapeutic effects against cancers (Choi *et al.*, 2022). The three benzimidazole-based

anticancer drugs are binimetinib, galeterone, and bendamustine (Figure 1.1). However, only bendamustine was approved for clinical use (Ponish *et al.*, 2013).

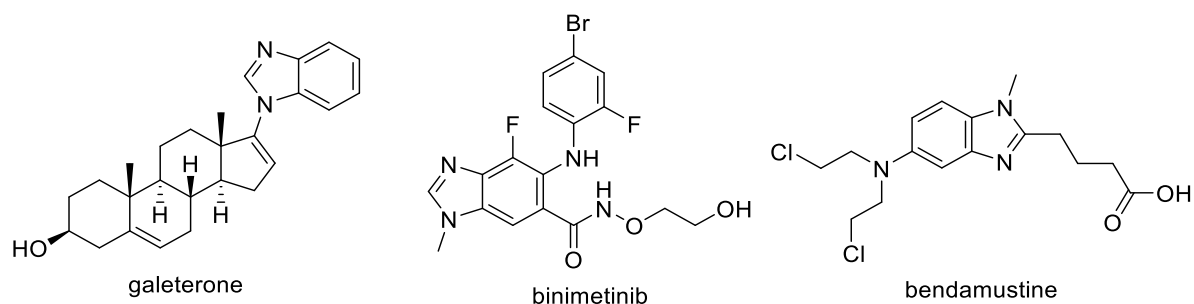


Figure 1.1: The three benzimidazole derived anticancer drugs: galeterone, binimetinib and bendamustine (Ponish *et al.*, 2013).

NHCs with an imidazole or benzimidazole moiety possess strong antibacterial or anticancer properties (Narasimhan *et al.*, 2011). In a recent study, Cevik and co-researchers synthesised and evaluated the cytotoxicity of a series *N*-allyl-*N'*-substituted benzimidazolium chlorides, (Figure 1.2) against the human breast (MCF7, MDA-MB-231) and prostate cancer cells (DU145). The anthracene-substituted homologue was the most active against all the tested cell lines: MDA-MB-231 ( $IC_{50} = 1.31 \mu M$ ), MCF7 ( $IC_{50} = 1.84 \mu M$ ) and DU145 ( $IC_{50} = 4.43 \mu M$ ). The potency of this compound was superior than those of *cis*-platin which one of the currently available chemotherapeutic agents. The results showed that the higher number of fused rings attached to the benzimidazole ring can be linked to the higher activities (Cevik *et al.*, 2020).

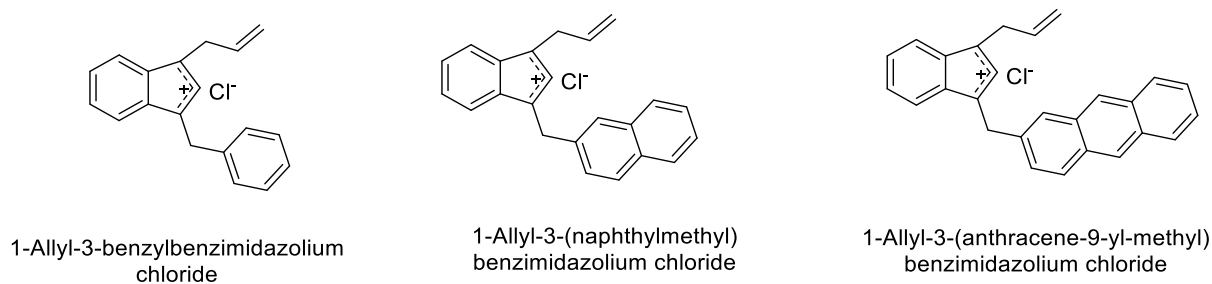


Figure 1.2: Bioactive *N*-Allyl-*N'*-substituted benzimidazolium chlorides (Cevik *et al.*, 2020).

Among the many metal-NHC complexes documented in the literature, Ag(I)-NHC complexes are the most well-known (Lin & Vasam, 2007; Lin & Vasam, 2004). Silver was commonly used to sustain human health. Silver salts were utilised by many civilizations to cleanse drinking water and treat wound infections (Teyssot *et al.*, 2009; Graham, 2005). However, one persistent issue with most silver-based medications is that they quickly lose activity as a result of the rapid release of Ag<sup>+</sup> ions (Melaiye *et al.*, 2005). However, this can be circumvented by using Ag(I)-NHC complexes. Site-specificity and gradual release of Ag<sup>+</sup> ions from these complexes distinguish them from other transition metal-based anticancer agents. The anticancer potentials of Ag(I)-NHC complexes can be easily modified by modifying the electronic and steric properties of the NHC ligands, which impact the complexes' hydrophilicity and lipophilicity (Johnson *et al.*, 2017; Marinelli *et al.*, 2016).

At molecular level, selenoenzymes thioredoxin reductase (TrxR) are small redox regulating proteins that maintain cellular redox homeostasis and cell survival. They are promising targets in anticancer treatments as TrxR are highly expressed in many cancers and often contribute to drug resistance. TrxR, a flavoprotein that is NADPH-dependent and closely linked to cancer, regulates cell homeostasis. A strong

correlation between this mitochondrial enzyme and antiproliferative activity has been established. Metal-NHC complexes were documented as TrxR inhibitors (Rubiani, 2010). For Au(I)-NHC complexes, a selenocysteine residue in the C-terminal active site of TrxR was reported to be the ultimate target. Covalent binding of gold ions to this site has been suggested as the mechanism of action of these cytotoxic complexes. In contrast, reports about TrxR inhibition of Ag(I)-NHC complexes are limited (Talbatov *et al.*, 2021).

The preparation and biological evaluation of new chemotherapeutics are costly and laborious. This can be overcome by rational design of lead compounds through the combination of computational chemistry and experimental studies. Computer-based methods such as molecular docking can predict the binding affinity of candidate chemotherapeutics to protein targets. It could change the way materials are designed so that it is based on cycles of computation, experimentation, and data analysis. This would speed up materials development and cut costs.

In light of the foregoing findings, we are inspired to synthesise two series of benzimidazolium derived *N,N'*-dialkylated NHC ligands and their Ag(I)-NHC complexes. They were characterized by FT-IR, <sup>1</sup>H- and <sup>13</sup>C-NMR spectroscopies and CHN elemental microanalysis. Their cytotoxic effects against human cervical cancer (HeLa) cells and normal skin fibroblasts (Hs27) were evaluated using the MTT assay. Possible binding interactions between the ligands and TrxR enzyme were predicted using molecular docking. Ligand with the highest binding affinity will be assayed against the TrxR enzyme to evaluate its inhibition potential.

## 1.2 Problem statement

The current platinum-based chemotherapeutics approved for clinical use have adverse toxic side effects, due to unselective apoptosis of cancerous and healthy cells. Hence, the development of selective and efficient metallodrugs is necessary. The choice of coordination metals and ligands are important in the design of new metallodrugs. Ligands that are easy to functionalise and form strong bonds with metals that maintain the entity of the drug unaffected along the metallodrug functioning (transport, solubility, stability) are preferred. In this context, *N*-heterocyclic carbenes (NHCs) are ideal candidates as they are easily functionalised, and form highly stable complexes with transition metals. Silver (Ag) salts have low toxicity and poses minimal risks to the human body, and Ag(I)-NHC complexes are promising effective surrogates for platinum-based chemotherapeutics due to their relatively low cytotoxicity to humans. However, the structural effects of the ligands on the cytotoxicity of the complexes remain unclear.

### 1.3 Research objectives

The study aims to:

- i. Synthesise and characterise two series of benzimidazolium derived *N,N'*-dialkylated NHC ligands and their silver(I)-NHC complexes using FT-IR and FT-NMR spectroscopies, and CHN elemental microanalysis.
- ii. Predict the molecular interactions of the NHC ligands and TrxR enzyme using molecular docking.
- iii. Evaluate the *in vitro* cytotoxic effects of the synthesised compounds against human cervical cancer (HeLa) cells and normal skin fibroblasts (Hs27) using the MTT assay.

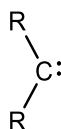


## CHAPTER 2

### LITERATURE REVIEW

#### 2.1 Carbenes

Carbene is a divalent carbon molecule that is neutral and has two unpaired electrons and six valence electrons. (Figure 2.1). The presence of the unpaired electrons (electron deficient) makes a carbene highly reactive and thus only exists as a labile and short-live intermediate in organic transformations. The first structural evidence for the formation of a dichloro carbene was discovered by Doering (von E. Doering & Hoffmann, 1954). In 1999, Arduengo reported the discovery of the first stable carbene (Arguendo, 1999).



R = H/alkyl/aryl

Figure 2.1: A general structure of a carbene

The highly reactive carbene carbon can adopt either a linear or bent geometry, depending on its hybridisation (Hahn & Jahnke, 2008). The majority of carbon atom in carbenes is  $sp^2$  hybridised, which means that the carbon atom is paired with a lone pair of electrons. Two of the three  $sp^2$  hybridised orbitals on a carbene carbon are used to form covalent bonds with other elements or atoms, and the lone pair of electrons can occupy either the  $sp^2$  hybridised orbital or the  $p$  orbital. There are two classes of carbene called singlet or triplet carbene depending on whether the non-bonding electrons are in the same or different orbitals (Figure 2.2). When two electrons are

placed in the same orbital, the carbene is known as a singlet carbene since the electron spins are in different directions. According to Hund's law, when electrons are positioned in various orbitals, parallel spin is favoured, and the resulting carbene is known as triplet carbene (Wiberg, 2004).

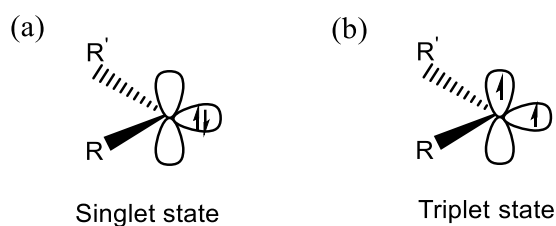


Figure 2.2: Electron spins in (a) a singlet carbene, and (b) a triplet carbene.

The electron spin state in carbenes is influenced by the type of substituents. In the ground state, carbenes are normally in the singlet states if the substituents attached to the carbene carbon are  $\sigma$ -electron withdrawing. The  $\sigma$ -orbital in the carbene carbon is stabilised inductively by electron withdrawing groups, which increases the energy difference between the  $\pi$ - and  $\sigma$ - orbitals. In contrast, if the substituents attached to the carbene carbon are  $\sigma$ -electron donating, the triplet carbene is favoured (Tomioka *et al.*, 1996; Hoffman *et al.*, 1968).

Carbenes are excellent nucleophiles and strong Lewis bases. They can bind with metals across the periodic table to form highly stable complexes (Arduengo *et al.*, 1991; Herrmann & Köcher, 1997; Öfele *et al.*, 1993). Fischer and Maasböl (Fischer and Maasböl, 1964) prepared the first stable Fischer carbene-tungsten complex in 1964. Fischer carbenes are versatile reagents which can produce metal complexes of low valency or low oxidation states. Fischer carbenes known as singlet carbenes accept

electron(s) via back donation ( $\pi$ -donation) from metals and transfer their electron pairs as  $\sigma$ -donation from the  $sp^2$  hybrid orbital (Figure 2.3 (a)). On the other hand, Schrock (Schrock, 1974) reported several Schrock carbene-tantalum complexes which are triplet carbenes that have two unpaired electrons which interact with metals to form two covalent bonds. These complexes were found to be nucleophilic because each of the covalent bonds was polarised toward the carbene carbon (Figure 2.3 (b)).

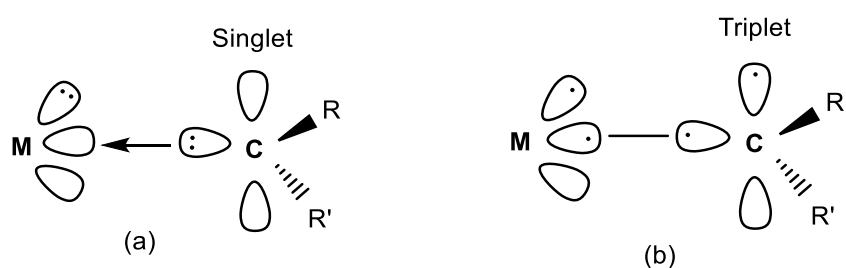
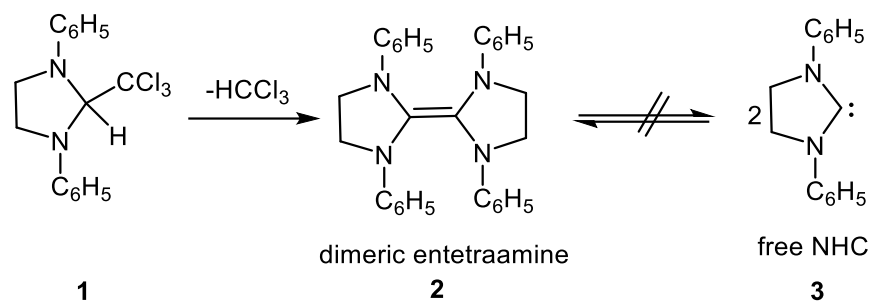


Figure 2.3: Carbene to metal bonding in (a) Fischer carbenes (Fischer and Maasböl, 1964) (b) Schrock carbenes (Schrock, 1974).

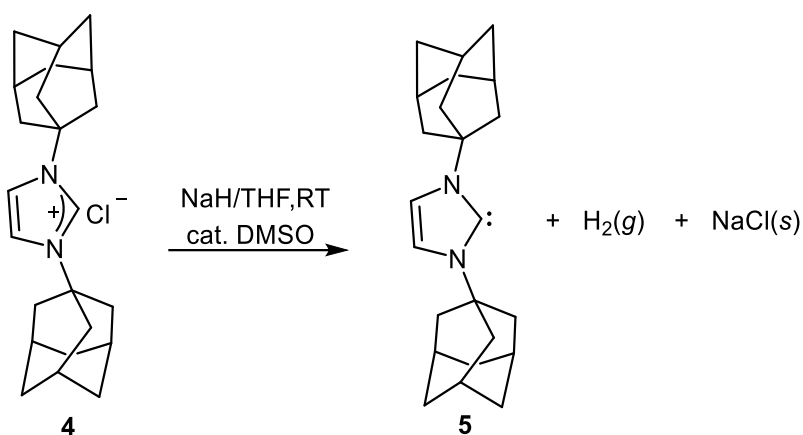
## 2.2 *N*-heterocyclic carbenes (NHCs)

In year 1960, Wanzlick (Wanzlick *et al.*, 1960) proposed that carbenes could be stabilized by electron donating effects from neighbouring nitrogen atoms in *N*-heterocyclic systems, and tried to isolate a free *N*-heterocyclic carbene (NHC) (**3**) from its precursor, *N, N'*-disubstituted imidazolidine (**1**) using thermal elimination reaction of chloroform. However, the attempt was unsuccessful. Instead, the dimeric form, entetramine (**2**) was obtained (Scheme 2.1). Further effect to cleave the C=C bond in entetramine by cross metathesis also failed leading him to proposed that **3** may be the intermediate of **2**, and postulated the presence of an equilibrium between these two compounds.



Scheme 2.1: Formation of a dimeric NHC, entetraamine, **2** from *N, N'*-disubstituted imidazolidine, **1** (Wanzlick *et al.*, 1960)

Inspired by Wanzlick's discovery, Arduengo and coworkers (Arduengo III *et al.*, 1991) isolated the first stable NHC in 1991. This NHC was prepared by deprotonation of bis(1-adamantyl)imidazolium chloride, **4** at room temperature in tetrahydrofuran with sodium hydride and a catalytic amount of dimethyl sulfoxide as a catalyst (Scheme 2.2). The carbene was discovered to exhibit exceptional stability at room temperature, and it was thoroughly characterised and crystallographically elucidated. Since then, NHCs have been established as very adaptable building blocks in the field of coordination chemistry. (Kascatan-Nebioglu *et al.*, 2007).



Scheme 2.2: The first isolable free NHC (Arguendo III *et al.*, 1991)

NHCs are cyclic singlet carbenes which contains two  $\pi$ -donating nitrogen atoms. The main stabilising forces come from the interactions between the lone electron pairs on nitrogen atoms and the  $\pi$  orbital in carbene carbon (Figure 2.4). The electronegative nitrogen atoms exert a negative inductive effect, which reduces the charge density on the carbene carbon, thus stabilising the NHC (Bourissou *et al.*, 2000). It was also postulated that NHC is stabilised via delocalization of electrons in the ring (Boehme & Frenking, 1996).

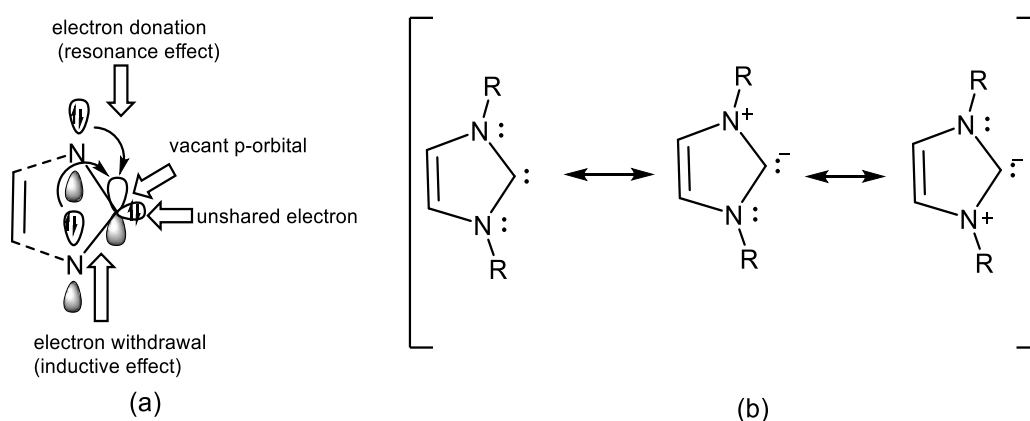


Figure 2.4: Stabilisation of NHCs via (a) electronegative inductive effects and (b) resonance (Bourissou *et al.*, 2000; Boehme & Frenking, 1996)

## 2.3 Synthesis of NHC precursor: azolium salts

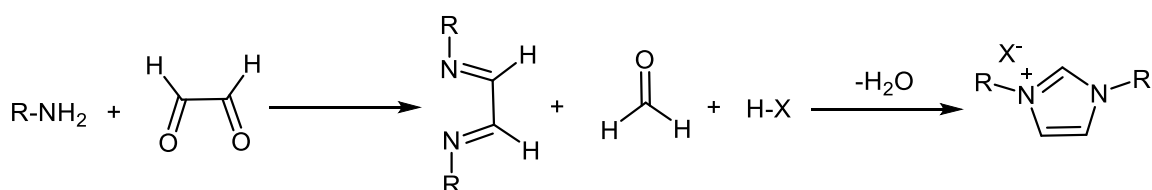
Since the discovery and isolation of the first free NHCs by Arduengo (Arduengo III *et al.*, 1991), several synthesis routes to prepare NHC precursors were developed. Imidazolium and benzimidazolium salts are the most common NHC precursors and hence, one of the most feasible methods of preparation of NHC is via the azolium salts route (Furstner *et al.*, 2006).

### 2.3.1. Condensation-Reduction Route

This route begins with the nucleophilic attack of two nitrogen atoms in ammonia (or an ammonia and an amine) on the carbonyl carbons of a dicarbonyl compound, followed by the removal of water molecules to yield the Schiff base. The formation of an imidazolium salt is the result of a condensation reaction between this Schiff base and an aldehyde. There are two distinct pathways that lead to the formation of the imidazolium salt (Hermann *et al.*, 2001).

#### (a) Synthesis of symmetrical imidazolium salts

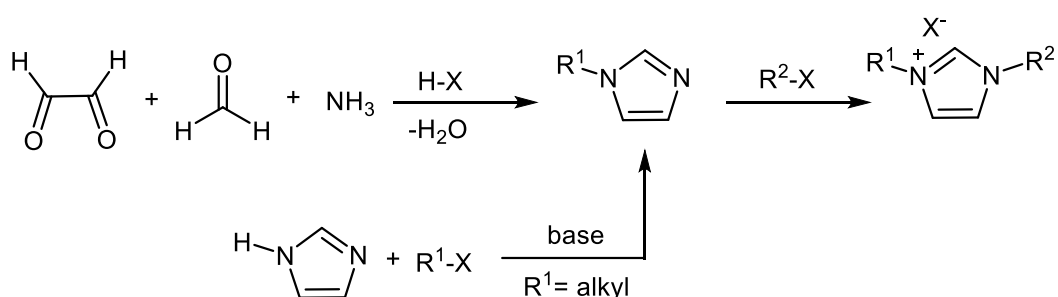
A two-step reaction can be used to synthesise symmetrical *N-N'*-disubstituted imidazolium salts, as shown in Scheme.2.3 (Bohm *et al.*, 2000). In the first step, a diimine is formed via condensation reaction of an aryl- or alkylamine with glyoxal. In the second step, condensation reaction of diimine with formaldehyde in the presence of a Brønsted acid yields the corresponding *N-N'*-imidazolium salt.



Scheme 2.3: Symmetric synthesis of imidazolium salts (Bohm *et al.*, 2000)

### (b) Synthesis of asymmetrical imidazolium salts

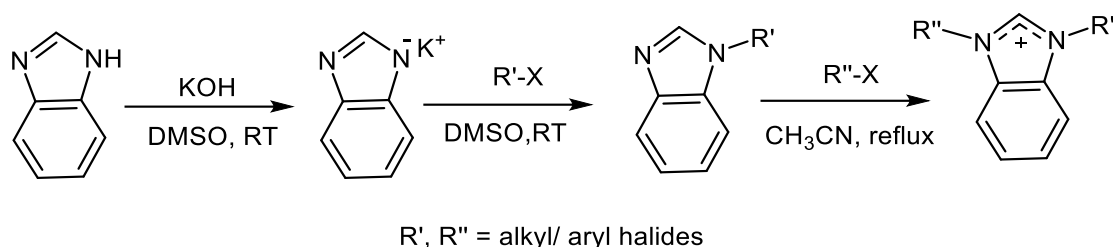
Asymmetrical imidazolium salts can be prepared similar to the symmetric synthesis via reaction of an amine with formaldehyde and glyoxal (Gridnev & Mihaltaseva, 1994). Preparation of asymmetrical imidazolium salts involved the cyclisation at pH 1 to form a *N*-alkyl-imidazolium salts. The other nitrogen atom was then alkylated in the presence of a base to yield the asymmetrically imidazolium salts (Scheme 2.4).



Scheme 2.4: Synthesis of asymmetrical imidazolium salts (Gridnev & Mihaltaseva, 1994)

### 2.3.2. Nucleophilic substitution at the azole heterocycles

Another route to synthesise symmetrical or asymmetrical NHC precursors is via alkylation of both nitrogen atoms in azole heterocycles (Scheme 2.5) (Starikova, *et al.*, 2003). This method afforded *N,N'*-dialkylated imidazolium and benzimidazolium salts in high yields.



Scheme 2.5: Synthesis of symmetrical or asymmetrical benzimidazolium salts  
(Starikova, *et al.*, 2003).

## 2.4 Benzimidazole as a NHC precursor

Benzimidazole is a planar, bicyclic compound made up of an imidazole ring fused with a benzene ring at the C-4 and C-5. The hydrogen atom can be attached to N-1 or N-3, thus giving benzimidazole two tautomeric forms, namely 1H- and 3H-benzimidazoles (Figure 2.5). Benzimidazole is a bioactive heterocyclic moiety. For example, reported that a naturally occurring benzimidazole derivative known as *N*-ribosyldimethylbenzimidazole functions as a cobalt axial ligand in vitamin B12. (Baker *et al.*, 1960). Benzimidazole is an important scaffold in medicines such as bendamustine, an anticancer drug and mebendazole, an anthelmintic drug (Kahveci *et al.*, 2015). A number of its organic derivatives are cytotoxic against various types of human cancers, such as colon cancer (Yadav *et al.*, 2018), leukemia (Sharma *et al.*, 2015), breast cancer (Yadav *et al.*, 2017), hepatocellular carcinoma (Refaat, 2015), and cervical cancer (Onnis *et al.*, 2016). Benzimidazolium salts are formed when both nitrogen atoms in benzimidazoles are substituted (Jakstell *et al.*, 2002). NHCs can be derived from these salts when a strong base removes an acidic proton from C-2 in this heterocycle.



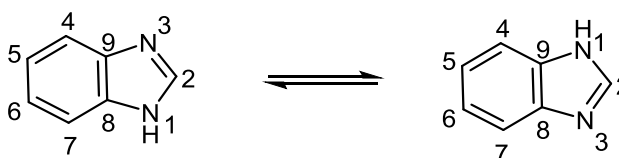
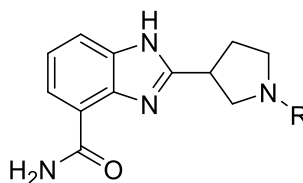


Figure 2.5: Benzimidazole tautomers.

In a recent study, Min and co-workers (Min *et al.*, 2019) reported a series of benzimidazole derivatives, **6a-6k** bearing different *N*-substituents (Figure 2.6), and their *in vitro* cytotoxicity against pancreatic adenocarcinoma cell lines (CAPAN-1) and breast carcinoma cell lines (MDA-MB-436). Compound **6i** was found to be the most potent against CAPAN-1 ( $IC_{50} = 11.4 \mu M$ ) and MDA-MB-436 ( $IC_{50} = 17.4 \mu M$ ). The half maximal inhibitory concentration,  $IC_{50}$  of these compounds were lower than those of the referenced drug, olaparib ( $IC_{50} > 100 \mu M$  (CAPAN-1), and  $0.041 > 100 \mu M$  (MDA-MB-436)).



- 6a** R = C<sub>9</sub>H<sub>11</sub>NO,    **6b** R = C<sub>10</sub>H<sub>13</sub>NO,  
**6c** R = C<sub>10</sub>H<sub>12</sub>O,    **6d** R = C<sub>10</sub>H<sub>10</sub>O,  
**6e** R = C<sub>12</sub>H<sub>13</sub>NO<sub>2</sub>,    **6f** R = C<sub>10</sub>H<sub>14</sub>O,  
**6g** R = C<sub>9</sub>H<sub>13</sub>N,    **6h** R = C<sub>11</sub>H<sub>14</sub>O<sub>2</sub>,  
**6i** R = C<sub>10</sub>H<sub>11</sub>ClO,    **6j** R = C<sub>4</sub>H<sub>11</sub>N,  
**6k** R = C<sub>3</sub>H<sub>9</sub>N

Figure 2.6: Benzimidazole derivatives with different *N*-substituents (Min *et al.*, 2019).

## 2.5 Metal-NHC complexes

NHCs are versatile ligands due to their ease of synthesis, functionalisation, isolation, as well as their ability to be metalated with a wide range of metals. Strong  $\sigma$ -donors characteristic of NHCs allows them to have highly nucleophilic carbene carbon atom, resulting in the formation of highly stable metal-NHC complexes. In general, NHCs are able to bind to metals through the donation of lone pairs of electrons to the empty  $d$  orbitals of metal centres, which results in the formation of powerful metal-ligand  $\sigma$ -bond. However, it is important to take into account the contribution of the metal-carbon  $\pi$  back bonding, even though  $\sigma$  donation is the primary component of the metal-ligand bond.

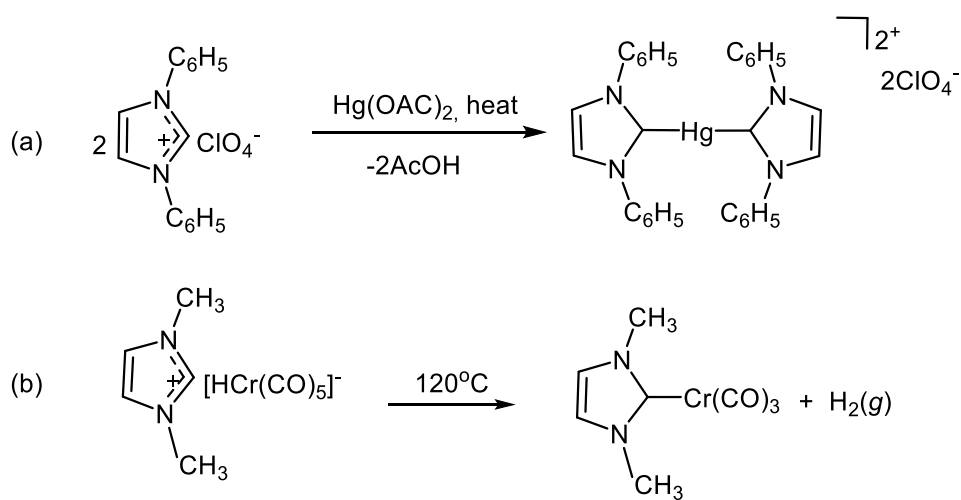
## 2.6 Preparation of metal-NHC complexes

NHCs are excellent  $\sigma$ -donor ligands, hence they form highly stable metal-NHC complexes with strong carbon-metal interactions (Arduengo *et al.*, 1991). Common preparation methods of metal-NHC complexes are: (i) *In situ* deprotonation of imidazolium and benzimidazolium salts with transition metal salts in basic media; (ii) reaction of free carbenes with metal precursors, and (iii) transmetalation with metal-NHC complexes (carbene transfer).

### 2.6.1 *In situ* deprotonation of imidazolium and benzimidazolium salts with metal salts

As early as 1968, Wanzlick and Öfele discovered NHC complexes with transition metal (Hg and Cr). Wanzlick and co-researchers (Wanzlick and Schönherr, 1968) prepared via *in situ* deprotonation of 1,3-diphenylimidazolium perchlorate using

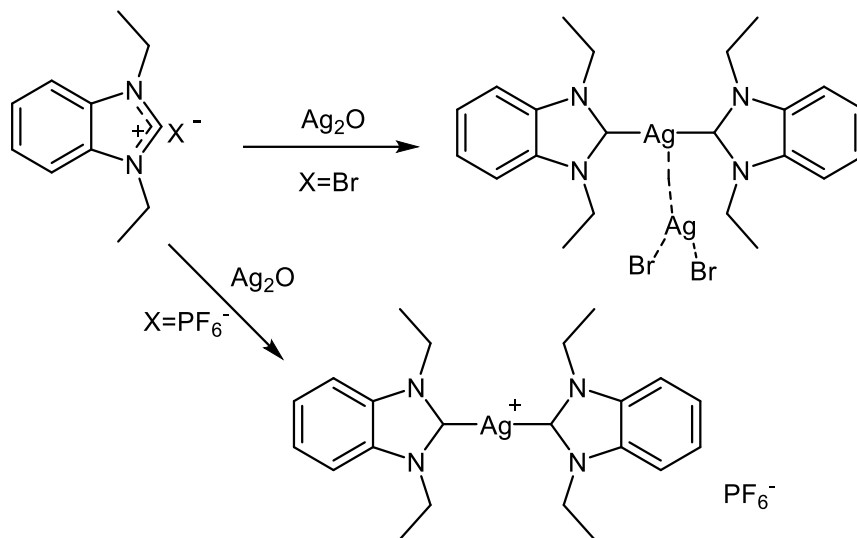
mercury(II) acetate to synthesise a mercury(II)-NHC complex. At the same time, Öfele (Öfele, 1968) attempted to synthesise 1,3-dimethylimidazolium pentacarbonylhydrochromate from hydrocarbonylmetalate (Scheme 2.6). They discovered that direct formation of a NHC-chromium complex was possible without the isolation of free carbene.



Scheme 2.6: Synthesis of the first NHC-transition metal complexes by (a) Wanzlick (Wanzlick and Schönherr, 1968) and (b) Öfele (Öfele, 1968).

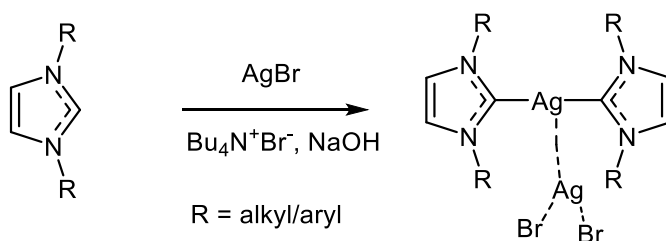
Deprotonation of azolium salts by metal salts such as silver(I) oxide ( $\text{Ag}_2\text{O}$ ) (Wang & Lin, 1998), silver acetate ( $\text{AgOAc}$ ) (Guerret, et al. 2000; Guerret, *et al.* 1997) and silver carbonate ( $\text{Ag}_2\text{CO}_3$ ) (Tulloch, *et al.* 2000) remains the most prevalent method in the syntheses of silver(I)-NHC complexes. The use  $\text{Ag}_2\text{O}$  in the synthesis of Ag(I)-NHC complexes of 1,3-diethylbenzimidazole-2-ylidenes was pioneered by Wang and Lin (1998) (Scheme 2.7). The use of this salt has several advantages. For example, metalation reactions with silver oxide can occur in air and at room temperature. They can also occur in various types of organic solvents. No excess base

is needed, and most of the time, deprotonation happens at C-2 of the benzimidazole ring.



Scheme 2.7: *In situ* deprotonation of azolium salts by  $\text{Ag}_2\text{O}$  to form silver(I)-NHC complexes (Wang & Lin, 1998).

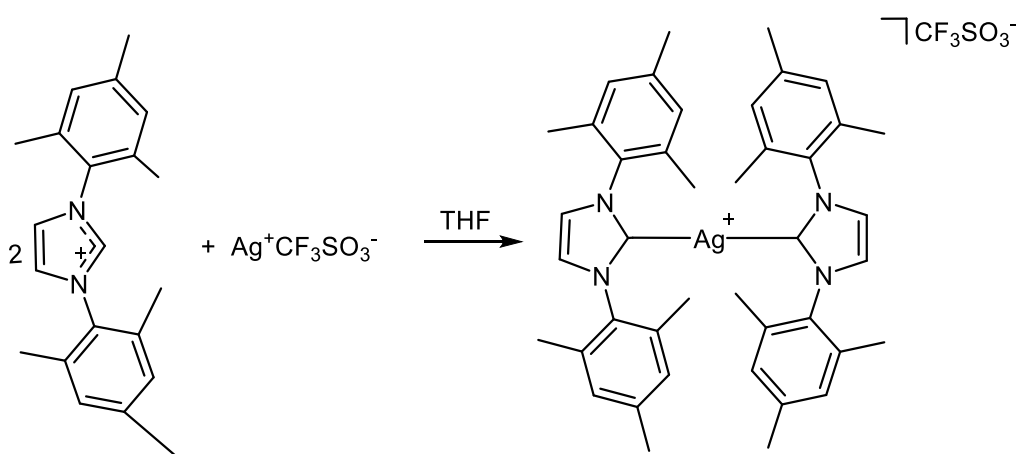
Another similar method which involved the use of basic phase transfer catalysts was reported by Tulloch and co-workers (2000). In the presence of silver bromide, these researchers prepared a bis  $\text{Ag}(\text{I})$ -NHC complex from imidazolium bromide using tetrabutylammonium bromide, a phase transfer catalyst. However, this technique could not be conducted with other imidazolium salts (Tulloch *et al.*, 2000).



Scheme 2.8: Synthesis of bis silver(I)-NHC complexes using a basic phase transfer catalyst (Tulloch *et al.*, 2000).

## 2.6.2 Reactions of free carbenes with metal precursors

The interaction of azolium salts with strong bases results in the formation of free carbenes. Arduengo prepared the first Ag(I)-NHC complex in 1993 by using the free carbene method (Arduengo, 1993). Deprotonation of an imidazolium salt, 1,3-dimesitylimidazol-2-ylidene by strong bases (KO<sup>t</sup>Bu or KH), and resulting the free carbene and silver triflate afforded a bis(carbene)-Ag(I) complex (Scheme 2.9). Since then, many Ag(I)-NHC complexes consisting of five, six and seven membered NHCs have been developed using this route (Lin *et al.*, 2013). One limitation of this method is the decomposition of complexes by strong bases.

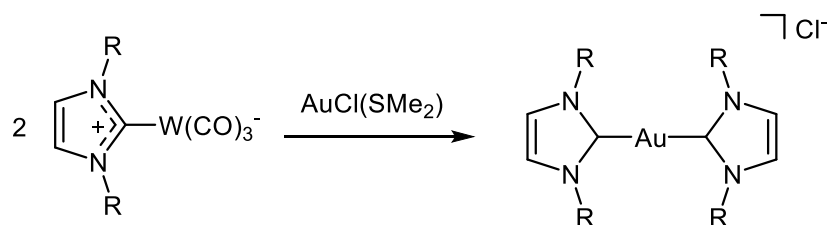


Scheme 2.9: Synthesis of the first silver(I)-NHC complex from 1,3-dimesitylimidazol-2-ylidene and silver(I)triflate (Arduengo, 1993).

## 2.6.3 Transmetalation or carbene transfer

Transmetalation is a type of organometallic reaction wherein a ligand is transferred from one metal to another. Fisher and Bech (1970) conducted the first study of carbene transfer between metal ions. Subsequently, Liu and co-workers (Liu *et al.*, 1998) devised another method for transmetalation to synthesis of Ag(I)-NHC

complexes. In this method Ag-NHC were synthesised from other metal-NHC complexes. In this study, the transition of W(0)-NHC complexes into Ag(I)-NHC complexes was verified by spectroscopy. However, Ag(I)-NHC complexes obtained from this method were moisture sensitive and disintegrated into salts when exposed to air. Apart from Ag(I)-NHC complexes, other stable metal-NHC complexes prepared from this method were reported (Scheme 2.10). This method remains useful till today to prepare Au-NHC and Pd-NHC complexes from Ag(I)-NHC (Ku, *et al.*, 1999).



Scheme 2.10: Transmetalation reaction from a W(0)-NHC complex to an Au(I)-NHC complex (Ku, *et al.*, 1999)

## 2.7 Biological activities of silver and its derivatives

Humans have been using metals since the dawn of time. The ancient Phoenicians, Greeks, Romans and Egyptians used silver metal in food preservation and water storage. This is because it can prevent the growth of bacteria and algae. Silver nitrate was mentioned by Paracelsus as an antiseptic for wound treatments long before 18<sup>th</sup> century. An important contribution was made in the 1881 by Carl Siegmund Franz Crede, who pioneered the use of 1% silver nitrate eye drop solution to protect newborn from ophthalmia neonatorum (Crede, 1881). Due to this success, this medicine is widely accepted throughout the world and used today.

Since 1840s, silver nitrate has been used to prevent infections in burn wounds, and its use has lasted till the 20<sup>th</sup> century. The use of silver nitrate was substantially decreased with the discovery and widespread use of antibiotics in the mid-20<sup>th</sup> century. However, the evolution of antibiotic-resistant bacteria has sparked renewed interest in silver-based antimicrobial agents. This led to the discovery of silver sulphadiazine by Fox in 1968 (Fox, 1974) (Figure 2.7). Antibiotics that contain silver have been shown to be effective against a variety of gram-positive and gram-negative bacteria (Melaiye *et al.*, 2004).

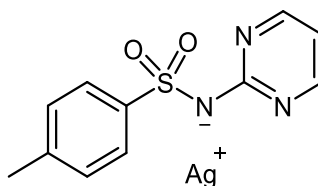
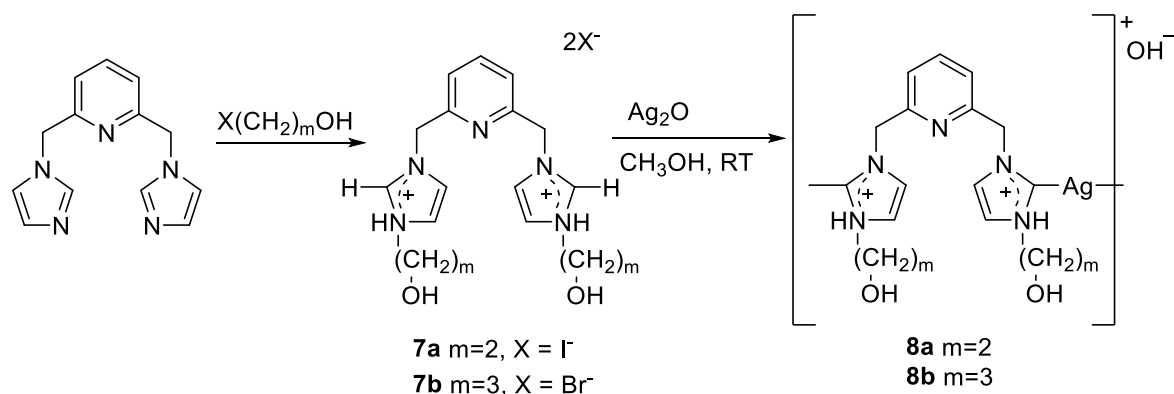


Figure 2.7: Silver sulfadiazine, a topical antibiotic.

### 2.7.1 Antimicrobial activities of Ag(I)-NHC complexes

The first antimicrobial activities of Ag(I)-NHC complexes were reported by Youngs and co-researchers (Youngs *et al.*, 2005). The pincer ligands **7a** and **7b** were synthesised by reacting 2,6-bis(imidazolomethyl)pyridine with 2-iodoethanol. Subsequently, by treating **7a** and **7b** with Ag<sub>2</sub>O in aqueous methanol, developed two water soluble pincer Ag(I)-NHC complexes, namely Ag(I)-2,6-bis(ethanolimidazolomethyl)pyridine hydroxide, **8a** and Ag(I)-2,6-bis(propanolimidazolomethyl)pyridine hydroxide, **8b** (Scheme 2.11). These complexes have stronger antimicrobial activities compared to silver nitrate against *Staphylococcus aureus*, *Pseudomonas aeruginosa*, and *Escherichia coli*. This could be due to the silver complexes were stabilised by the pincer ligands, thus reducing the

rate of release of  $\text{Ag}^+$  ions which prolonged their antimicrobial effect (Melaiye *et al.*, 2004).



Scheme 2.11: Synthesis of **7a-b** and **8a-b** from 2,6-bis(imidazolomethyl)pyridine (Youngs *et al.*, 2004).

Kaloğlu and co-workers (Kaloğlu *et al.*, 2016) reported a series of benzimidazolium-derived  $\text{Ag}(\text{I})$ -NHC complexes, **9a-9c** that showed high antimicrobial activities against *S. aureus*, *E. coli*, *P. aeruginosa* and *Enterococcus faecalis*. The presence of electron-donating and bulky groups attached to the nitrogen atoms in the NHC ligand was found to enhance the antimicrobial activities of these complexes. The MIC values of the complexes ranged from 6.25 - 50  $\mu\text{g}/\text{mL}$  which were superior to that of the standard drugs, namely fluconazole, ciprofloxacin and ampicillin (MIC = 0.39 - 3.12  $\mu\text{g}/\text{mL}$ ). Complex **9c** was the most active against the bacterial strains with MICs ranging from 6.25 - 12.5  $\mu\text{g}/\text{mL}$  (Figure 2.8).



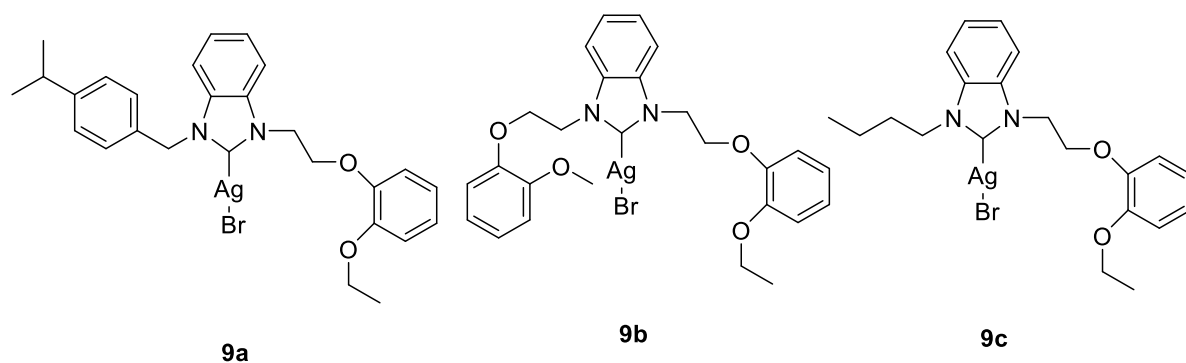
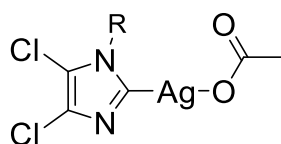


Figure 2.8: Bioactive benzimidazolium derived Ag(I)-NHC complexes, **9a-9c**

(Kaloğlu, *et al.*, 2016).

### 2.7.2 Anticancer activities of Ag(I)-NHC complexes

Youngs and co-workers (Youngs *et al.*, 2005) pioneered in the field of anticancer research involving Ag(I)-NHC complexes. The *in vitro* cytotoxicity of mono-ligand Ag(I)-NHC complexes derived from 4,5-dichloro-1H-imidazolium salts, **10a-10c** (Figure 2.9) against breast cancer (MB157), ovarian cancer (OVCAR-3), and cervical cancer (HeLa) cell lines. These complexes were active against MB157 and OVCAR-3 ( $IC_{50}$  ranged from 8 - 25  $\mu M$ ) but inactive against HeLa cells ( $IC_{50}$  values > 200  $\mu M$ ). However, their anticancer activities were lower than that of cisplatin ( $IC_{50}$  12 - 25  $\mu M$ ).



**10a**, R=methyl

**10b**, R=hexyl

**10c**, R=-CH<sub>2</sub>-naphthalene

Figure 2.9: Imidazolium derived Ag(I)-NHC complexes with anticancer properties

(Youngs *et.al.*, 2005).